

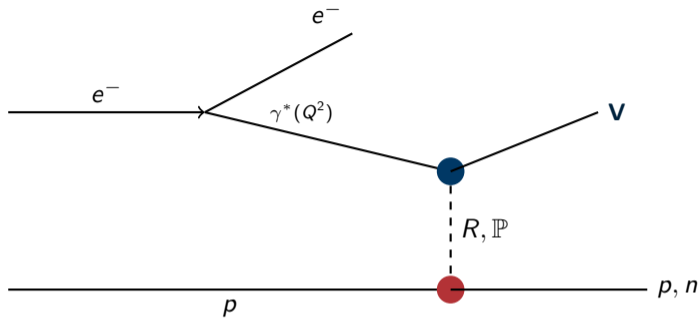
# A Model-Independent Partial Wave Approach to Meson Photo- and Electroproduction

Spherical Harmonic Moments, Spin Density Matrices, Partial Wave Amplitudes

Derek Glazier  
Dillon Leahy with JPAC

CLAS Collaboration Meeting June 26

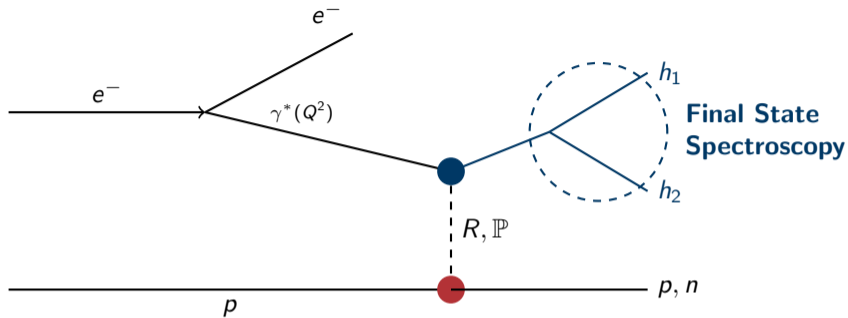
# Electron Scattering Experiments



## Physics Mapping Overview

- Electroproduction allows us to isolate different physics regimes by selecting specific kinematic regions and focusing on different parts of the scattering diagram.
- Same amplitude formalism underlies all physics aspects.
- Hadron spectroscopy and deep processes are just different projections of same processes.

# Electron Scattering Experiments

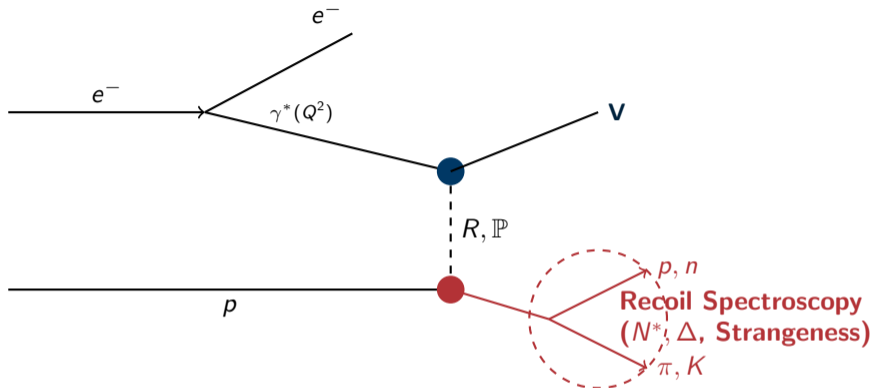


## Hadron Spectroscopy (Meson)

Study of the produced system ( $V$ ) via its decay products.

- **Concepts:** Resonance pole extraction (Mass, Width),  $J^{PC}$  quantum numbers, photocouplings.
- **Methods:** Partial Wave Analysis (PWA) of decay angular distributions.

# Electron Scattering Experiments

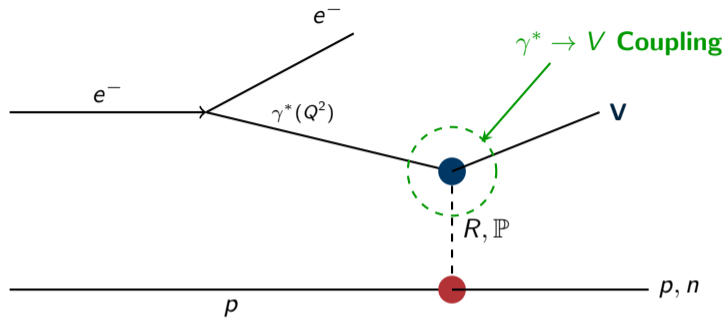


## Baryon Spectroscopy (Recoil Decay)

The nucleon target is excited into a resonance ( $N^*, \Delta$ ) which subsequently decays into a meson-baryon final state.

- **Concepts:** Baryon resonance pole positions.
- **Goal:** Mapping the excitation spectrum of the nucleon and searching for missing resonances.
- **Note:** Requires extension to include baryon decay amplitudes.

# Electron Scattering Experiments

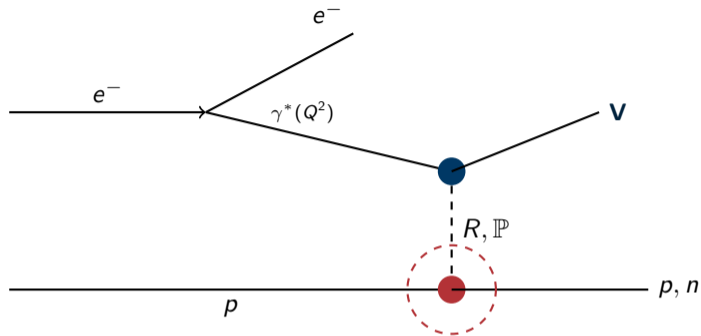


## Hadron Structure (Meson)

Focuses on the production vertex to probe how the virtual photon couples to hadronic matter and the internal quark-gluon makeup.

- **Concepts:** Meson Form Factors ( $F_\pi(Q^2)$ ), Distribution Amplitudes (DAs).
- **Goal:** Understanding the transition from non-perturbative to perturbative QCD.

# Electron Scattering Experiments



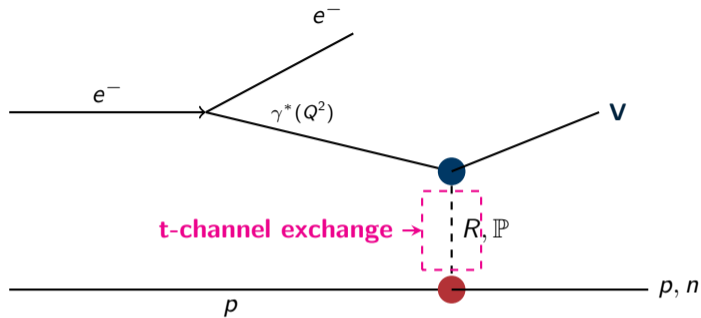
## Nucleon Context

### Hadron Structure (Baryon)

Analyzes the response of the nucleon at the lower vertex to understand its 3D internal landscape.

- **Concepts:** Generalized Parton Distributions (GPDs), Nucleon Form Factors ( $G_E, G_M$ ).
- **Goal:** Tomography of the nucleon (spatial and momentum distributions).
- **Requirements:** Polarised beam and transverse and longitudinal targets.
- **?:** role of Regge picture in interpreting hard processes.

# Electron Scattering Experiments

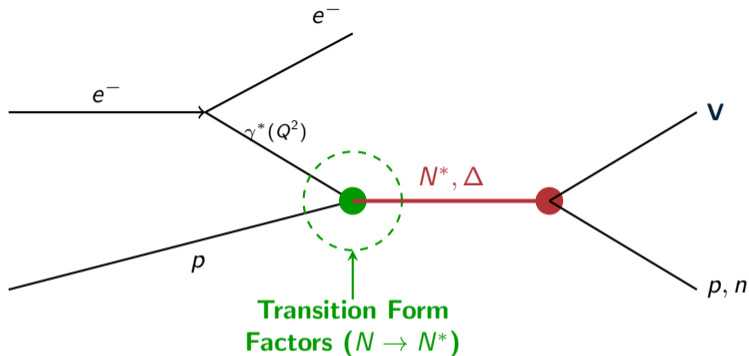


## Regge Structure

Examines the nature of the  $t$ -channel exchange mediating the interaction between the two vertices.

- **Concepts:** Regge Trajectories  $\alpha(t)$ , Pomeron vs. Reggeon exchange.
- **Goal:** Understanding the high-energy gluonic “glue” ( $\mathbb{P}$ ) and meson trajectories ( $R$ ).

# Electron Scattering Experiments

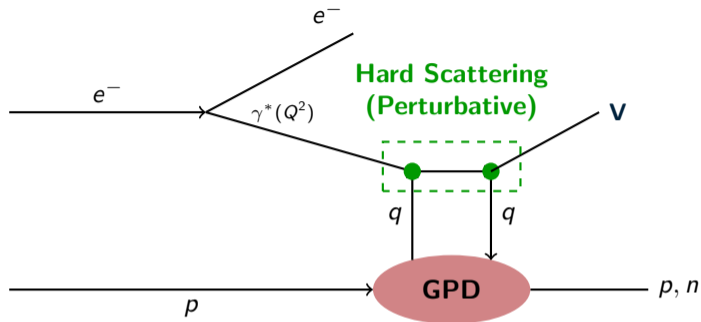


## s-Channel Resonance Production (CLAS12 Focus)

At CLAS12 kinematics (lower  $W$ ), the  $\gamma^*$  and target nucleon can fuse directly into an s-channel resonance before decaying.

- **Concepts:**  $N \rightarrow N^*$  Transition Form Factors, Electroexcitation dependence on  $Q^2$ .
- t-distribution  $\rightarrow$  complex  $\theta_{CM}$  dependence based on contributing resonances.
- **Goal:** Probing the internal structure of excited baryon states directly from the initial coupling.

# Electron Scattering Experiments



## Deeply Virtual Processes (Handbag Diagram)

At high  $Q^2$ , the interaction factorizes into a hard perturbative process (photon interacting with a single quark) and a soft non-perturbative part (encoded in GPDs).

- **Concepts:** Deeply Virtual Meson Production (DVMP), Handbag factorization.
- **Goal:** Accessing the 3D partonic structure by isolating single-quark interactions.
- **Requirements:** High  $Q^2$  and large  $W$  to ensure the validity of factorization.

# Experimental Considerations

- For all physics topics, the **same experimental observables** should be measured to ensure consistency.
- In particular, when the number of final state hadronic particles is  $N > 2$ , we must properly integrate over decay angles. This is strictly required for:
  - Proper **acceptance correction** in cross section measurements.
  - Proper averaging of **Single Spin Asymmetries**.

## The Optimal Solution: SDMEs

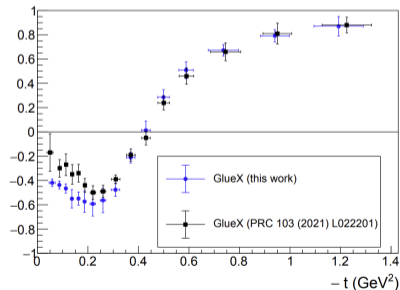
The simplest and most rigorous solution is to measure **Spin Density Matrix Elements (SDMEs)**.

- They contain the **maximal information** extractable from the experiment.
- **Recommendation:** This should be standard practice for **all CLAS measurements** where  $N > 2$ .

Example: Photon Asymmetries for GlueX  $\Delta^{++}$

Comparison of extraction methods:

- **Black:** via Asymmetry
- **Blue:** via SDMEs



# Starting Point: CLAS 2009 $\pi^+\pi^-$ Moments Analysis

PRL **102**, 102001 (2009)

PHYSICAL REVIEW LETTERS

week ending  
13 MARCH 2009

## Measurement of Direct $f_0(980)$ Photoproduction on the Proton

M. Battaglieri,<sup>1</sup> R. De Vita,<sup>1</sup> A. P. Szczepaniak,<sup>2</sup> K. P. Adhikari,<sup>34</sup> M. Aghasyan,<sup>19</sup> M. J. Amarian,<sup>34</sup> P. Ambrozewicz,<sup>14</sup> M. Anghinolfi,<sup>3</sup> G. Asryan,<sup>47</sup> H. Avakian,<sup>41</sup> H. Bagdasaryan,<sup>34</sup> N. Baillie,<sup>46</sup> J. P. Ball,<sup>4</sup> N. A. Baltzell,<sup>40</sup> V. Baturine,<sup>26,41</sup>

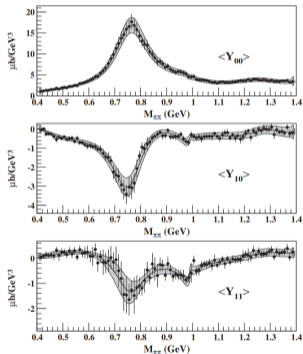


Fig A: Extracted angular moments  $\langle Y_{00} \rangle$ ,  $\langle Y_{10} \rangle$ , and  $\langle Y_{11} \rangle$  mapping the clear  $S$ - $P$  interference profiles.

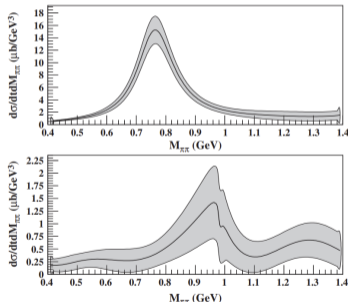


Fig B: Resulting PWA cross sections cleanly splitting the small scalar  $S$ -wave from the dominant vector  $P$ -wave.

## Defining Angular Moments

$$\langle Y_{LM} \rangle = \sqrt{4\pi} \int d\Omega_\pi Y_{LM} \frac{d^3\sigma}{dt dM_{\pi\pi} d\Omega_\pi}$$

## Disentangling $S$ and $P$ Waves

- **Overlap:** The  $\pi^+\pi^-$  final state contains overlapping  $S$  and  $P$  wave amplitudes.
- **Scale Limit:** Direct scalar extraction is buried because the vector  $P$ -wave ( $\rho$ ) cross section is  $\sim 50\times$  larger.
- **Resolution:** Moments preserve the phase interference terms (e.g.,  $\langle Y_{10} \rangle$ ), allowing PWA to isolate the  $f_0(980)$ .
- model dependent due to unpolarised photon beam

# Photoproduction Formalism: Intensity Decomposition & $\alpha$ Definition

## Moments of angular distribution and beam asymmetries in $\eta\pi^0$ photoproduction at GlueX

[V. Mathieu](#)<sup>1,2,\*</sup>, [M. Albaladejo](#)<sup>1,†</sup>, [C. Fernández-Ramírez](#)<sup>3</sup>, [A.W. Jackura](#)<sup>4,5</sup>, [M. Mikhasenko](#)<sup>6</sup>, [A. Pilloni](#)<sup>7,8</sup>, and [A.P. Szczepaniak](#)<sup>1,4,5</sup> (Joint Physics Analysis Center)

The total differential cross section for two-spinless-meson photoproduction with an elliptically polarized photon beam splits into independent angular intensity components:

### Total Intensity Decomposition

$$\mathcal{I}(\Omega, \Phi) = \mathcal{I}^0(\Omega) - P_L \mathcal{I}^1(\Omega) \cos(2\Phi) - P_L \mathcal{I}^2(\Omega) \sin(2\Phi) - P_C \mathcal{I}^3(\Omega)$$

### Explicit Definition of the Beam Configuration Index $\alpha$

The superscript  $\alpha \in \{0, 1, 2, 3\}$  tracks the physical polarization operators acting on the photon density matrix :

Index $\alpha$	Observable Component	Physical Beam State	Polarization Operator
$\alpha = 0$	$\mathcal{I}^0(\Omega)$	Unpolarized Beam Frame Baseline	Identity Matrix $\mathbf{1}$
$\alpha = 1$	$\mathcal{I}^1(\Omega)$	Linear Polarization ( $\cos 2\Phi$ modulation)	Pauli Matrix $\sigma_x$
$\alpha = 2$	$\mathcal{I}^2(\Omega)$	Linear Polarization ( $\sin 2\Phi$ modulation)	Pauli Matrix $\sigma_y$
$\alpha = 3$	$\mathcal{I}^3(\Omega)$	Circular Polarization Element	Pauli Matrix $\sigma_z$

<sup>1</sup>

<sup>1</sup>Extension required for  $V \rightarrow$  any. e.g.  $\pi + \rho$ ;  $e^+ + e^-$ ; ...

# Photoproduction Formalism: Reflectivity Amplitudes

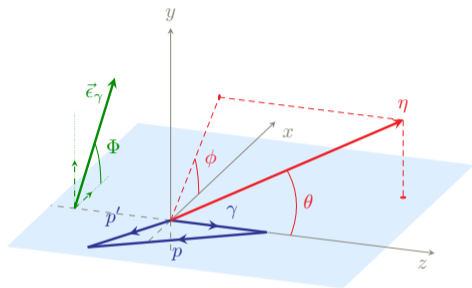


**Figure:** Gottfried-Jackson coordinate system configuration. The z-axis follows the incoming beam ( $\gamma$ ), and the xz production plane contains the target ( $p$ ) and recoil ( $p'$ ) nucleon trajectories .

Opposite reflectivities do not interfere and sum completely incoherently inside the observable matrix blocks, block-diagonalizing the parameter space .

To exploit parity conservation and isolate independent exchange naturalities, we transform the straight photon helicity production amplitudes  $T_{\lambda_\gamma, m}$  into the reflectivity basis  $[l]_m^{(\epsilon)}$ :

## Reflectivity Basis Definition

$$[l]_m^{(\epsilon)} = \frac{1}{\sqrt{2}} (T_{+1, m} - \epsilon(-1)^m T_{-1, -m})$$

## Physical Interpretation of Quantities

- **Reflectivity ( $\epsilon = \pm 1$ ):** Characterizes reflection symmetry across the production plane. In the high-energy Regge limit, it cleanly separates exchanges of good naturality ( $P = \epsilon(-1)^J$ )
- **Meson Orbital Spin ( $\ell$ ):** Represents the total angular momentum  $J$  of the two-spinless-meson decay system.
- **Spin Projection ( $m$ ) & Flips:** Tracks the meson spin projection along the quantization z-axis. The number of helicity flips is invariant between bases, :  $\Delta\lambda = |m - \lambda_\gamma|$  for transverse photons.

# Photoproduction Formalism: Spherical Harmonic Decomposition

Each distinct directional intensity component  $\mathcal{I}^\alpha(\Omega)$  is expanded directly into orthogonal spherical harmonics to isolate the model-independent moments  $H^\alpha(LM)$ :

## Spherical Harmonic Expansion

$$\mathcal{I}^\alpha(\Omega) = \kappa \sum_{L,M} H^\alpha(LM) Y_L^M(\Omega)$$

**NOTE** : These spherical harmonic moments summarize the most complete and general information that can be extracted from such an experiment.

## Spin-Density Matrix Elements (SDMEs) to Partial Waves

The matrix elements are constructed as bilinear combinations of the underlying reflectivity partial-wave amplitudes  $[\ell]_m^{(\epsilon)}$ :

$$\rho_{mm'}^{0,\ell\ell'} = [\ell]_m^{(\epsilon)} [\ell']_{m'}^{(\epsilon)*} + (-1)^{m-m'} [\ell]_{-m}^{(\epsilon)} [\ell']_{-m'}^{(\epsilon)*}$$

$$\rho_{mm'}^{1,\ell\ell'} = -\epsilon \left( (-1)^m [\ell']_{-m}^{(\epsilon)} [\ell]_{m'}^{(\epsilon)*} + (-1)^{m'} [\ell]_m^{(\epsilon)} [\ell']_{-m'}^{(\epsilon)*} \right)$$

$$\rho_{mm'}^{2,\ell\ell'} = -i\epsilon \left( (-1)^m [\ell']_{-m}^{(\epsilon)} [\ell]_{m'}^{(\epsilon)*} - (-1)^{m'} [\ell]_m^{(\epsilon)} [\ell']_{-m'}^{(\epsilon)*} \right)$$

$$\rho_{mm'}^{3,\ell\ell'} = [\ell]_m^{(\epsilon)} [\ell']_{m'}^{(\epsilon)*} - (-1)^{m-m'} [\ell]_{-m}^{(\epsilon)} [\ell']_{-m'}^{(\epsilon)*}$$

# Photoproduction Formalism: Classic Schilling & Wolf Projections

For an isolated pure vector state ( $J = 1$ , such as intermediate  $\rho(770) \rightarrow \pi^+\pi^-$  decay), the explicit geometric angular expansions for the four beam configurations map strictly onto the classic SDME basis  $\rho_{mm'}^\alpha$ :

## Truncated $P$ -Wave Intensity Angular Projections

$$\mathcal{I}^0(\theta, \phi) = \frac{3}{4\pi} \left[ \frac{1}{2}(1 - \rho_{00}^0) + \frac{1}{2}(3\rho_{00}^0 - 1) \cos^2 \theta - \sqrt{2} \operatorname{Re}[\rho_{10}^0] \sin 2\theta \cos \phi - \rho_{1-1}^0 \sin^2 \theta \cos 2\phi \right]$$

$$\mathcal{I}^1(\theta, \phi) = \frac{3}{4\pi} \left[ \rho_{11}^1 \sin^2 \theta + \rho_{00}^1 \cos^2 \theta - \sqrt{2} \operatorname{Re}[\rho_{10}^1] \sin 2\theta \cos \phi - \rho_{1-1}^1 \sin^2 \theta \cos 2\phi \right]$$

$$\mathcal{I}^2(\theta, \phi) = \frac{3}{4\pi} \left[ \sqrt{2} \operatorname{Im}[\rho_{10}^2] \sin 2\theta \sin \phi + \operatorname{Im}[\rho_{1-1}^2] \sin^2 \theta \sin 2\phi \right]$$

$$\mathcal{I}^3(\theta, \phi) = \frac{3}{4\pi} \left[ \sqrt{2} \operatorname{Im}[\rho_{10}^3] \sin 2\theta \sin \phi + \operatorname{Im}[\rho_{1-1}^3] \sin^2 \theta \sin 2\phi \right]$$

*Note: The angles  $\theta$  and  $\phi$  define the direction of the decay products inside the Gottfried-Jackson rest frame .*

# Photoproduction Formalism: Mapping Moments to Classic SDMEs

By comparing moments with S+W, we arrive at the exact algebraic dictionary linking experimental Moments  $H^\alpha(LM)$  to the classic vector-meson SDMEs (when  $H^0(0,0) \equiv 1$ ):

## Classic SDMEs Extracted from Moments

$$\begin{aligned}\rho_{00}^0 &= \frac{1}{3} (5H^0(2,0) + 1) & \rho_{1-1}^1 &= \frac{5}{\sqrt{6}} H^1(2,2) \\ \rho_{1-1}^0 &= -\frac{5}{\sqrt{6}} H^0(2,2) & \text{Re}[\rho_{10}^1] &= -\frac{5}{\sqrt{12}} H^1(2,1) \\ \text{Re}[\rho_{10}^0] &= \frac{5}{\sqrt{12}} H^0(2,1) & \text{Im}[\rho_{1-1}^2] &= \frac{5}{\sqrt{6}} H^2(2,2) \\ \rho_{00}^1 &= -\frac{1}{3} H^1(0,0) - \frac{5}{3} H^1(2,0) & \text{Im}[\rho_{10}^2] &= -\frac{5}{\sqrt{12}} H^2(2,1) \\ \rho_{11}^1 &= -\frac{1}{3} H^1(0,0) + \frac{5}{6} H^1(2,0) & \text{Im}[\rho_{1-1}^3] &= \frac{5}{\sqrt{6}} H^3(2,2) \\ & & \text{Im}[\rho_{10}^3] &= -\frac{5}{\sqrt{12}} H^3(2,1)\end{aligned}$$

**Note:** Spin-density matrix elements (SDMEs) as per the Diehl notation can be calculated directly from these Schilling and Wolf (S+W) SDMEs.

# Electroproduction Formalism: 9-Component Intensity Expansion

When moving to virtual photons ( $Q^2 > 0$ ), the introduction of longitudinal polarization expands the virtual-photon spin-density matrix into nine independent Hermitian response blocks ( $\alpha = 0, \dots, 8$ ):

## Full Virtual Lepton-Hadron Angular Intensity

$$\begin{aligned} I(\Omega, \Phi) = & I^0(\Omega) + \epsilon I^4(\Omega) - P_T I^1(\Omega) \cos 2\Phi - P_T I^2(\Omega) \sin 2\Phi \\ & + P_{T'} I^3(\Omega) - P_{LT} I^5(\Omega) \cos \Phi - P_{LT} I^6(\Omega) \sin \Phi \\ & + P_{LT'} I^7(\Omega) \cos \Phi + P_{LT'} I^8(\Omega) \sin \Phi \end{aligned}$$

## General Formulation of the Observables

Each individual beam response component  $I^\alpha(\Omega)$  expands directly into spherical harmonic moments  $H^\alpha(LM)$  without truncation:

$$I^\alpha(\Omega) = s_\alpha \sum_{L,M} \sqrt{\frac{2L+1}{4\pi}} H^\alpha(LM) Y_L^M(\Omega) \quad \text{where} \quad s_\alpha = \begin{cases} 1 & \text{if } \alpha \in \{0, 4\} \\ -1 & \text{otherwise} \end{cases}$$

The moments map linearly to the underlying density matrix via fixed Clebsch-Gordan coefficients:

# Electroproduction Formalism: Virtual Photon Reflectivity Amplitudes

To maintain parity conservation and isolate independent exchange naturalities at  $Q^2 > 0$ , we separate the production amplitudes into Transverse ( $T$ ) and Longitudinal ( $L$ ) sectors within the reflectivity basis ( $\epsilon = \pm 1$ ):

## Reflectivity Amplitudes Formulation

$$[\ell]_{Tm}^\epsilon = \frac{1}{2} \left( T_{+1,m}^\ell - \epsilon(-1)^m T_{-1,-m}^\ell \right)$$

$$[\ell]_{Lm}^\epsilon = \frac{1}{2} \left( T_{0,m}^\ell + \epsilon(-1)^m T_{0,-m}^\ell \right)$$

## Physical Definition of Amplitudes Quantum Numbers

- **Reflectivity ( $\epsilon = \pm 1$ ):** Characterizes the reflection symmetry across the production plane to cleanly isolate exchange naturalities in the Regge limit. Opposite reflectivities sum completely incoherently within the observables.
- **Meson Orbital Spin ( $\ell$ ):** Dictates the total angular momentum  $J$  of the produced two-body meson decay system.
- **Spin Projection ( $m$ ):** Quantifies the projection of the meson spin along the quantization  $z$ -axis inside the Gottfried-Jackson frame.

# Electroproduction Formalism: Pure Transverse & Longitudinal Blocks

Operating in the general case without wave truncation, the diagonal photon response classes decompose directly into bilinear products of the reflectivity amplitudes  $[\ell]_{X,m}^\epsilon$ :

## Pure Transverse Matrix Blocks ( $\alpha = 0, 1, 2, 3$ )

$$\rho_{mm'}^{0,\ell\ell'} = \frac{\kappa}{2} \sum_{\epsilon} \left( [\ell]_{Tm}^\epsilon ([\ell']_{Tm'}^{\epsilon,*}) + (-1)^{m'-m} [\ell]_{T,-m}^\epsilon ([\ell']_{T,-m'}^{\epsilon,*}) \right)$$

$$\rho_{mm'}^{1,\ell\ell'} = -\frac{\kappa}{2} \sum_{\epsilon} \epsilon \left( (-1)^m [\ell]_{T,-m}^\epsilon ([\ell']_{Tm'}^{\epsilon,*}) + (-1)^{m'} [\ell]_{Tm}^\epsilon ([\ell']_{T,-m'}^{\epsilon,*}) \right)$$

$$\rho_{mm'}^{2,\ell\ell'} = -\frac{i\kappa}{2} \sum_{\epsilon} \epsilon \left( (-1)^m [\ell]_{T,-m}^\epsilon ([\ell']_{Tm'}^{\epsilon,*}) - (-1)^{m'} [\ell]_{Tm}^\epsilon ([\ell']_{T,-m'}^{\epsilon,*}) \right)$$

$$\rho_{mm'}^{3,\ell\ell'} = \frac{\kappa}{2} \sum_{\epsilon} \left( [\ell]_{Tm}^\epsilon ([\ell']_{Tm'}^{\epsilon,*}) - (-1)^{m'-m} [\ell]_{T,-m}^\epsilon ([\ell']_{T,-m'}^{\epsilon,*}) \right)$$

## Pure Longitudinal Matrix Block ( $\alpha = 4$ )

$$\rho_{mm'}^{4,\ell\ell'} = \kappa \sum_{\epsilon} [\ell]_{Lm}^\epsilon ([\ell']_{Lm'}^{\epsilon,*})$$

**Note:** The longitudinal response  $\alpha = 4$  maps uniquely to longitudinal photon transitions ( $[\ell]_L$ ). While the incoming virtual photon carries zero helicity ( $\lambda_{\gamma^*} = 0$ ), the final hadronic states retain their full, untruncated spin projections  $m$  and  $m'$ .

# Electroproduction Formalism: Longitudinal-Transverse Interferences

The off-diagonal cross-talk terms represent interference blocks constructed from mixed products of Transverse ( $T$ ) and Longitudinal ( $L$ ) modes. They split cleanly into unpolarized and polarized electron beam sectors:

## Unpolarized Lepton Beam Interferences ( $\alpha = 5, 6$ )

$$\rho_{mm'}^{5,\ell\ell'} = \frac{\kappa}{2\sqrt{2}} \sum_{\epsilon} \left( [l]_{Lm}^{\epsilon} ([\ell']_{Tm'}^{-\epsilon,*}) + [l]_{Tm}^{\epsilon} ([\ell']_{Lm'}^{-\epsilon,*}) + (-1)^{m'-m} \left[ [l]_{L,-m}^{\epsilon} ([\ell']_{T,-m'}^{-\epsilon,*}) + [l]_{T,-m}^{\epsilon} ([\ell']_{L,-m'}^{-\epsilon,*}) \right] \right)$$
$$\rho_{mm'}^{6,\ell\ell'} = -\frac{\kappa}{2\sqrt{2}} \sum_{\epsilon} \left( [l]_{Lm}^{\epsilon} ([\ell']_{Tm'}^{-\epsilon,*}) + [l]_{Tm}^{\epsilon} ([\ell']_{Lm'}^{-\epsilon,*}) + (-1)^{m'-m} \left[ [l]_{L,-m}^{\epsilon} ([\ell']_{T,-m'}^{-\epsilon,*}) + [l]_{T,-m}^{\epsilon} ([\ell']_{L,-m'}^{-\epsilon,*}) \right] \right)$$

## Polarized Lepton Beam Interferences ( $\alpha = 7, 8$ )

$$\rho_{mm'}^{7,\ell\ell'} = \frac{\kappa}{2\sqrt{2}} \sum_{\epsilon} \left( [l]_{Lm}^{\epsilon} ([\ell']_{Tm'}^{-\epsilon,*}) + [l]_{Tm}^{\epsilon} ([\ell']_{Lm'}^{-\epsilon,*}) - (-1)^{m'-m} \left[ [l]_{L,-m}^{\epsilon} ([\ell']_{T,-m'}^{-\epsilon,*}) + [l]_{T,-m}^{\epsilon} ([\ell']_{L,-m'}^{-\epsilon,*}) \right] \right)$$
$$\rho_{mm'}^{8,\ell\ell'} = \frac{\kappa}{2\sqrt{2}} \sum_{\epsilon} \left( [l]_{Lm}^{\epsilon} ([\ell']_{Tm'}^{-\epsilon,*}) - [l]_{Tm}^{\epsilon} ([\ell']_{Lm'}^{-\epsilon,*}) + (-1)^{m'-m} \left[ [l]_{L,-m}^{\epsilon} ([\ell']_{T,-m'}^{-\epsilon,*}) - [l]_{T,-m}^{\epsilon} ([\ell']_{L,-m'}^{-\epsilon,*}) \right] \right)$$

Note: Amplitudes  $[l]$  on the left inside the bilinear products track wave  $\ell$ , while those on the right track wave  $\ell'$ .

# Relating Moments to Cross Sections

Experimentally, the purely transverse and longitudinal fluxes are combined unless separated via Rosenbluth techniques. One directly measures the photon polarization-weighted moment sum:  $H^{04}(LM) = H^0(LM) + \epsilon H^4(LM)$ .

## Unpolarized 5-Fold Differential Cross Section

$$\frac{d^5\sigma}{dQ^2 dW dt dm d\Phi} = \Gamma(Q^2, W) \left\{ \frac{d^2\sigma_T}{dt dm} + \epsilon \frac{d^2\sigma_L}{dt dm} + \epsilon \cos(2\Phi) \frac{d^2\sigma_{TT}}{dt dm} \right. \\ \left. + \sqrt{2\epsilon(1+\epsilon)} \cos(\Phi) \frac{d^2\sigma_{LT}}{dt dm} + h_e \sqrt{2\epsilon(1-\epsilon)} \sin(\Phi) \frac{d^2\sigma_{LT'}}{dt dm} \right\}$$

## Parity Conservation & Missing Terms

Integrating over the solid angle  $d\Omega$  isolates the  $L = 0, M = 0$  scalar moments:  $\int I^\alpha(\Omega) d\Omega = s_\alpha H^\alpha(00)$ .

**Result:** For an unpolarized target and recoil ( $\beta = \delta = 0$ ), parity dictates  $S_\alpha = +1$ . Responses with  $S_\alpha = -1$  ( $\alpha \in \{2, 3, 6, 7\}$ ) have analytically vanishing  $M = 0$  states.

Their associated imaginary cross-sections

$(\sigma_{TT}^{\sin 2\Phi}, \sigma_{TT'}, \sigma_{LT}^{\sin \Phi}, \sigma_{LT'}^{\cos \Phi})$  are therefore strictly zero.

## Mapping the Surviving Moments

$$\sigma_T = H^0(00) \quad \sigma_L = H^4(00)$$

$$\sigma_{TT} = H^1(00) \quad \sigma_{LT} = H^5(00)$$

$$\sigma_{LT'} = H^8(00)$$

# Experimental Extraction and Normalization

Unbinned Extended Maximum Likelihood fits and other methods provide a set of *unscaled* relative moments,  $\hat{H}^\alpha(LM)$ . To extract absolute cross sections, these fitted shapes must be scaled to the total experimental yield.

## 1. Fit Normalization Convention

We conventionally normalize the unscaled moments so the total unpolarized scalar component sums exactly to 2:

$$\hat{H}^{04}(00) = \hat{H}^0(00) + \epsilon \hat{H}^4(00) = 2$$

## 2. Global Yield Constraint

The acceptance-corrected event yield in a kinematic bin  $\Delta V$  is related to the integrated luminosity  $\mathcal{L}$  and photon flux  $\bar{\Gamma}$ :

$$N_{\text{events}} = \mathcal{L} \cdot \Delta V \cdot \bar{\Gamma} \int_0^{2\pi} d\Phi \int d\Omega I(\Omega, \Phi)$$

Integrating out the azimuth  $\Phi$  kills interference terms, isolating the true physical scalar moments:

## 3. The Absolute Scale Factor ( $\mathcal{N}$ )

Because true moments are proportional to fitted moments ( $H^\alpha = \mathcal{N} \hat{H}^\alpha$ ), substituting the fit convention yields the exact scale factor:

$$\mathcal{N} = \frac{N_{\text{events}}}{4\pi \cdot \mathcal{L} \cdot \Delta V \cdot \bar{\Gamma}}$$

*Note: The  $4\pi$  denominator arises naturally from the combination of the  $2\pi$  azimuthal integral and the sum-to-2 fit convention.*

## 4. Final Cross Section Extraction

Multiplying the extracted scalar moments by this kinematic scale factor yields the absolute differential cross sections isolated from the fit:

$$\frac{d^2\sigma^\alpha}{dt dm} = \mathcal{N} \cdot \hat{H}^\alpha(00)$$

# Summary: Why Shift to the Reflectivity PWA Framework?

Transitioning from legacy density matrix parameters to an unconstrained reflectivity partial-wave analysis yields a substantial physics payoff at both vertices of the interaction:

## 1. Unraveling Hadronic Spectroscopy

- **Arbitrary Spin Extension:** Natively expands to accommodate arbitrary produced meson spins, moving past simple pure  $J = 1$  vector truncations.
- **Disentangling Overlapping States:** Resolves and isolates states of different spins decaying simultaneously into the exact same final state channels.
- **Direct SDME Construction:** Provides an explicit algebraic formulation to calculate traditional Schilling-Wolf or Diehl SDMEs directly from the amplitudes.
- **Clean Parity Filtering:** Natively block-diagonalizes the equations, cleanly separating natural ( $\epsilon = +1$ ) and unnatural ( $\epsilon = -1$ ) exchange categories in the Regge picture.

## 2. Unlocking 3D Nucleon Structure

- **Strict Model Independence:** Reflectivity partial waves are model independent quantities, extracting clean observables free of hadronic production model assumptions.
- **Optimized  $L/T$  Separation:** Under  $t$ -channel Regge factorization no interference with top/bottom vertices. This isolates  $\sigma_L$  and  $\sigma_T$  from a single unpolarized energy dataset.
- **Polarised  $L/T$  Separation:** regain model independence when include polarised targets or recoil
- **Direct Translation to GPDs:** Isolated partial waves map directly to Compton Form Factors (CFFs), acting as exact quantum filters for the vector ( $H, E$ ) and axial-vector ( $\tilde{H}, \tilde{E}$ ) GPD families.

# Moments to Partial Wave Amplitudes: The Inversion Procedure

## Real Moments ( $H^0, H^1$ )

$$H^0(2, 0) = \frac{2}{5} \sum_{\epsilon=\pm} (2|P_0^\epsilon|^2 - |P_{+1}^\epsilon|^2 - |P_{-1}^\epsilon|^2)$$

$$H^1(0, 0) = 2 \sum_{\epsilon=\pm} \epsilon (|P_0^\epsilon|^2 - 2|P_{+1}^\epsilon||P_{-1}^\epsilon| \cos \Delta\phi_{+1,-1}^\epsilon)$$

$$H^1(2, 0) = \frac{4}{5} \sum_{\epsilon=\pm} \epsilon (|P_0^\epsilon|^2 + |P_{+1}^\epsilon||P_{-1}^\epsilon| \cos \Delta\phi_{+1,-1}^\epsilon)$$

$$H^0(2, 1) = \frac{2\sqrt{3}}{5} \sum_{\epsilon=\pm} (|P_{+1}^\epsilon||P_0^\epsilon| \cos \Delta\phi_{+1,0}^\epsilon - |P_0^\epsilon||P_{-1}^\epsilon| \cos \Delta\phi_{0,-1}^\epsilon)$$

$$H^1(2, 1) = \frac{2\sqrt{3}}{5} \sum_{\epsilon=\pm} \epsilon (|P_{+1}^\epsilon||P_0^\epsilon| \cos \Delta\phi_{+1,0}^\epsilon - |P_0^\epsilon||P_{-1}^\epsilon| \cos \Delta\phi_{0,-1}^\epsilon)$$

$$H^0(2, 2) = -\frac{2\sqrt{6}}{5} \sum_{\epsilon=\pm} |P_{+1}^\epsilon||P_{-1}^\epsilon| \cos \Delta\phi_{+1,-1}^\epsilon$$

$$H^1(2, 2) = \frac{\sqrt{6}}{5} \sum_{\epsilon=\pm} \epsilon (|P_{+1}^\epsilon|^2 + |P_{-1}^\epsilon|^2)$$

## Imaginary Moments ( $H^2, H^3$ )

$$H^2(2, 1)/i = \frac{2\sqrt{3}}{5} \sum_{\epsilon=\pm} \epsilon (-|P_{+1}^\epsilon||P_0^\epsilon| \cos \Delta\phi_{+1,0}^\epsilon - |P_0^\epsilon||P_{-1}^\epsilon| \cos \Delta\phi_{0,-1}^\epsilon)$$

$$H^2(2, 2)/i = \frac{\sqrt{6}}{5} \sum_{\epsilon=\pm} \epsilon (|P_{-1}^\epsilon|^2 - |P_{+1}^\epsilon|^2)$$

$$H^3(2, 1)/i = \frac{2\sqrt{3}}{5} \sum_{\epsilon=\pm} (|P_{+1}^\epsilon||P_0^\epsilon| \sin \Delta\phi_{+1,0}^\epsilon + |P_0^\epsilon||P_{-1}^\epsilon| \sin \Delta\phi_{0,-1}^\epsilon)$$

$$H^3(2, 2)/i = \frac{2\sqrt{6}}{5} \sum_{\epsilon=\pm} |P_{+1}^\epsilon||P_{-1}^\epsilon| \sin \Delta\phi_{+1,-1}^\epsilon$$

## Numerical Inversion via MINUIT

The estimator matches experimental data against the partial-wave functional definitions:

$$\chi^2 = \sum_{\alpha, L, M} \frac{\left( H_{\text{exp}}^\alpha(LM) - H_{\text{calc}}^\alpha(LM)(\ell, m, \epsilon) \right)^2}{\sigma_{\alpha, LM}^2}$$

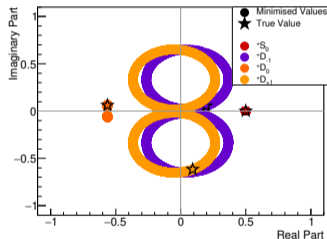
⇒ **Amplitudes:**  $||[\ell]_m^\epsilon|$  (Moduli tracker) **Phases:**  $\phi_m^\epsilon$

**Note:** We just show the example P-wave only. Similar sets of moments equations exist for all partial wave combinations.

# Numerical Example: Photoproduction

Numerical inversion of the moment equations for an illustrative  $S$  and  $D$ -wave system demonstrates how increasing the polarization configuration ( $\alpha$ ) systematically eliminates mathematical degeneracies. We can determine the amplitudes as we have more observables (polarized moments) than real numbers from PW amplitudes.

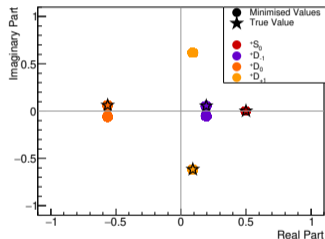
## 1. Unpolarized ( $H^0$ )



### Continuous Ambiguity

The system of equations is under-constrained, resulting in an infinite family of valid solutions forming continuous bands.

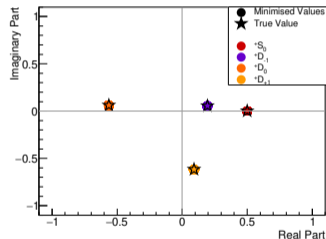
## 2. Linear ( $H^0, H^1, H^2$ )



### Discrete Ambiguity

Linear observables provide enough constraints to collapse the continuous bands down to exactly **two discrete complex conjugate states**.

## 3. Elliptical ( $H^0, H^1, H^2, H^3$ )

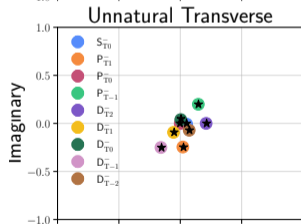
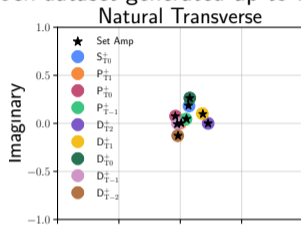


### Unique Solution

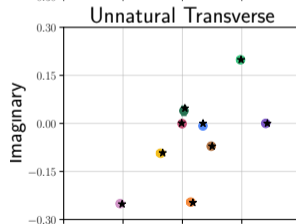
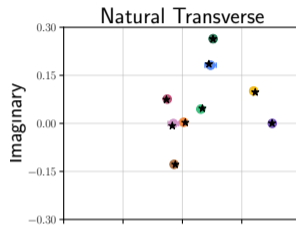
Adding circular polarization ( $H^3$ ) constrains the imaginary phase domains ( $\sin \Delta\phi$ ), breaking the mirror symmetry to reveal a **single, unique solution**.

# Numerical Example: Electroproduction (Transverse Sectors)

A fixed-amplitude closure study demonstrates the stability and uniqueness of the numerical inversion using a mock dataset generated up to  $D$ -waves ( $\ell_{max} = 2$ ) :



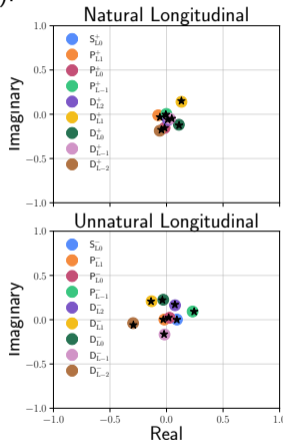
Full Parameter Space: Transverse sectors extracted cleanly.



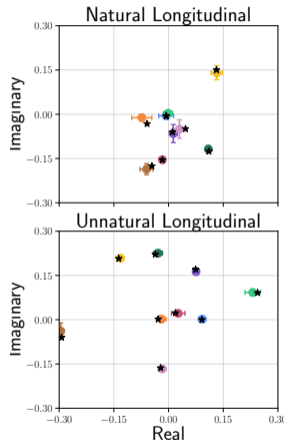
Zoomed Resolution Verification: Lack of false solution branches.

# Numerical Example: Electroproduction (Longitudinal Sectors)

And the longitudinal sectors, where the fit basis remains highly overconstrained (31 equations for 20 parameters):



Full Parameter Space: Longitudinal sectors extracted cleanly.



Zoomed Resolution Verification: High-resolution convergence space mapping.

## Amplitude Level $L/T$ Separation

- Traditional longitudinal-transverse ( $\sigma_L/\sigma_T$ ) separation requires a Rosenbluth scan, necessitating costly beam energy changes.
- **Our Assumption:** By invoking  $t$ -channel **Regge Factorization**, the upper virtual-photon vertex factorizes cleanly from the lower nucleon vertex.

### The Vertex Factorization Theorem

$$[I]_{cm;k}^\epsilon(Q^2, t, m) = \mathcal{V}_{\text{top}}^{c,\epsilon}(Q^2) \cdot \mathcal{D}_I(m) \cdot \mathcal{V}_{\text{bottom}}^\epsilon(t, k)$$

### The Mathematical Extraction Advantage

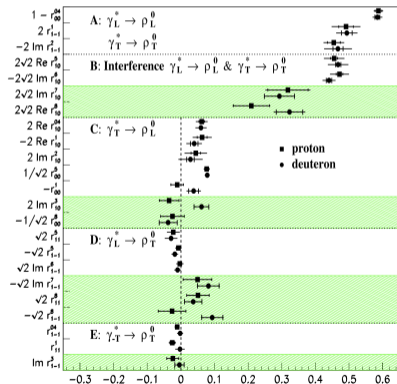
Because the target-nucleon piece  $\mathcal{V}_{\text{bottom}}^\epsilon$  carries **no dependence** on the photon's polarization state ( $c \in \{T, L\}$ ), the relative phases of the target helicity sum are identical across the longitudinal and transverse sectors. Coherence is preserved in the  $LT$  interference terms, allowing an **extraction of partial wave amplitudes and thereby absolute  $\sigma_L$  and  $\sigma_T$  from a single unpolarized energy.**

# Application to existing unpolarised target data

## Spin density matrix elements in exclusive $\rho^0$ electroproduction on $^1\text{H}$ and $^2\text{H}$ targets at 27.5 GeV beam energy

Regular Article – Experimental Physics | [Open access](#) | Published: 17 July 2009

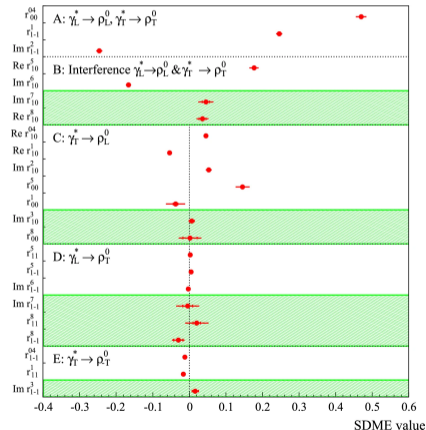
Volume 62, pages 659–695 (2009) | [Cite this article](#)



## Spin density matrix elements in exclusive $\rho^0$ meson muoproduction

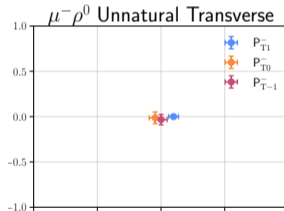
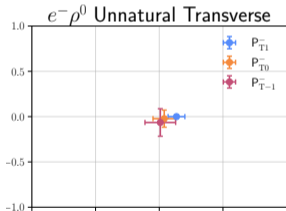
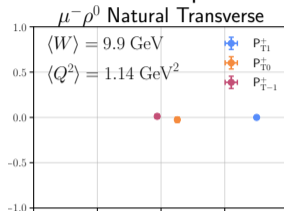
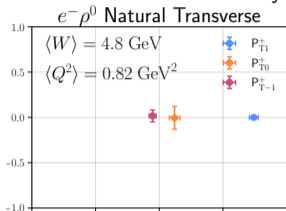
Regular Article – Experimental Physics | [Open access](#) | Published: 13 October 2023

Volume 83, article number 924 (2023) | [Cite this article](#)



# Real-World Data: $\rho^0$ Production (Transverse Sectors)

Applying the unconstrained reflectivity PWA numerical inversion to historical experimental data



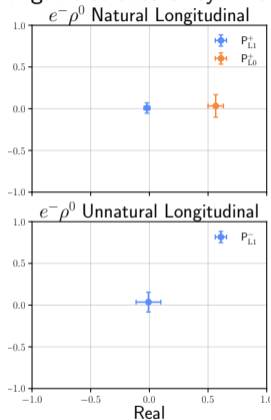
**Electron Production:** Extracted  $e^- \rho^0$  transverse amplitudes .

**Muon Production:** Extracted  $\mu^- \rho^0$  transverse amplitudes.

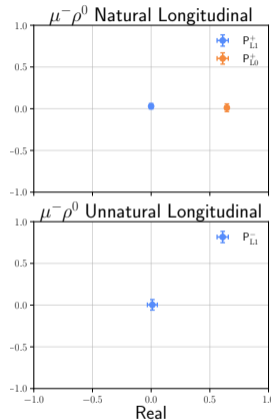
**Observation:** Both independent datasets display structural agreement, dominated by a highly prominent Natural Transverse  $m = 1$  no-helicity-flip amplitude ( $[\ell]_{T1}^+$ ) signifying expected Pomeron/Reggeon exchange trajectories.

# Real-World Data: $\rho^0$ Production (Longitudinal Sectors)

The corresponding longitudinal sector extractions illustrate clean isolation of the primary diffractive structures alongside structural symmetry constraints :



**Electron Production:** Extracted  $e^- \rho^0$  longitudinal amplitudes.

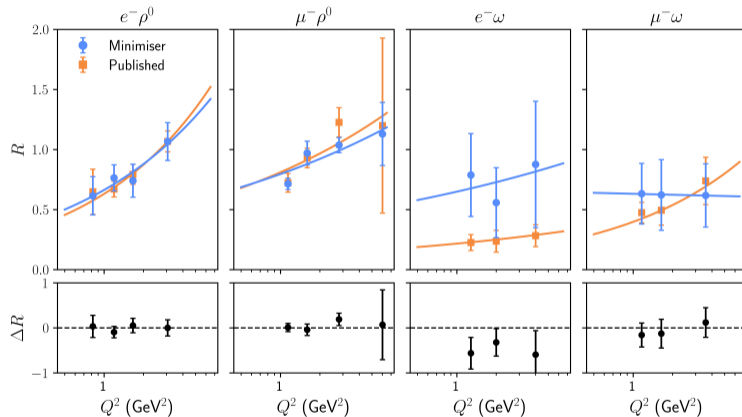


**Muon Production:** Extracted  $\mu^- \rho^0$  longitudinal amplitudes.

**Key Observation:** The longitudinal sector shows clear dominance of the Natural Longitudinal  $m = 0$  non-helicity-flip wave( $[\ell]_{L0}^+$ ) which relates to twist 2 GPDs.

# Experimental Results: Longitudinal-to-Transverse Ratio $R$

The extracted ratio of longitudinal to transverse cross sections,  $R = \sigma_L/\sigma_T$  can now be calculated directly from the partial wave amplitudes



## Direct Amplitude Derivation

$R$  for  $\rho$  agrees well with published results, while for  $\omega$  we see more significant differences due to contribution from unnatural pion pole term.

# Complete Tensor Polarization: Accounting for Full Nucleon Spin

## Intensity to amplitudes

### 1. Global Angular Intensity (Measured Cross Section):

$$I(\Omega, \Phi; \mathbf{S}_I, \mathbf{S}_R) = \sum_{\alpha=0}^8 \sum_{\beta=0}^3 \sum_{\delta=0}^3 P_{\alpha\beta\delta}(\Phi, \mathbf{S}_I, \mathbf{S}_R) I^{\alpha\beta\delta}(\Omega)$$

### 2. Decomposition into Component Intensities (Projected Moments):

$$I^{\alpha\beta\delta}(\Omega) = s_{\alpha\beta\delta} \sum_{L,M} \sqrt{\frac{2L+1}{4\pi}} H^{\alpha\beta\delta}(LM) Y_L^M(\Omega)$$

### 3. Extraction of Model-Independent Moments: - experimentally measurable quantities

$$H^{\alpha\beta\delta}(LM) = s_{\alpha\beta\delta} \sum_{\ell, \ell', m, m'} \left( \frac{2\ell'+1}{2\ell+1} \right)^{1/2} C_{\ell 0}^{\ell' 0} C_{\ell m}^{\ell' m'} \rho_{mm'}^{\alpha\beta\delta, \ell\ell'}$$

### 4. Bilinear Production Amplitude Decomposition (Helicity Tensors):

$$\rho_{mm'}^{\alpha\beta\delta, \ell\ell'} = \kappa \sum_{\Lambda} T_{\lambda m; \lambda_1 \lambda_2}^{\ell} \Sigma_{\lambda \lambda'}^{\alpha} \sigma_{\lambda_1 \lambda'_1}^{\beta} \sigma_{\lambda'_2 \lambda_2}^{\delta} T_{\lambda' m'; \lambda'_1 \lambda'_2}^{\ell' *}$$

## Polarisation Matrices

- $\alpha$ : Photon Matrix  $\Sigma^{\alpha}$
- $\beta$ : Initial Nucleon  $\sigma^{\beta}$
- $\delta$ : Recoil Nucleon  $\sigma^{\delta}$

$$s_{\alpha\beta\delta} = \begin{cases} 1 & \alpha \in \{0, 4\}, \beta = \delta = 0 \\ -1 & \text{otherwise} \end{cases}$$

- $\Lambda = \{\lambda, \lambda', \lambda_1, \lambda'_1, \lambda_2, \lambda'_2\}$ : Collective helicity indices
- $\lambda, \lambda'$ : Photon projection  $(\pm 1, 0)$  ·  $\lambda_1, \lambda'_1$ : Initial nucleon
- $\lambda_2, \lambda'_2$ : Recoiling baryon
- $P_{\alpha\beta\delta}$ : Combined polarisation direction

- $\Phi$  lepton/hadron plane
- $S_I^{\beta}$  spin of initial proton
- $S_R^{\delta}$  spin of final baryon
- $\Omega = (\theta, \phi)$ : Meson Decay angles

# Electroproduction Formalism: Reduced Nucleon $k$ -Basis

The virtual-photon parity relation allows us to collapse the four initial-recoil spin lines into just two independent sectors:

## Parity Reduction to $k$ -Basis

Using the common parity rule across photon sectors:

$$[\ell]_{Xm;-\lambda_1,-\lambda_2}^\epsilon = \epsilon(-1)^{\lambda_1-\lambda_2} [\ell]_{Xm;\lambda_1,\lambda_2}^\epsilon$$

We define two independent canonical states ( $k \in \{-1, +1\}$ ):

$$k = +1 \equiv [\ell]_{Xm;++}^\epsilon \quad \text{(Non-Flip)}$$

$$k = -1 \equiv [\ell]_{Xm;+-}^\epsilon \quad \text{(Flip)}$$

The remaining states are fixed by parity completion:

$$[--] = \epsilon[+1], \quad [-+] = -\epsilon[-1]$$

## The Algebraic Advantage

- **Standard SDME Extraction:** Treats elements as independent variables, heavily inflating fit dimensionality.
- **PWA  $k$ -Basis Extraction:** Natively enforces parity, angular momentum.

## The Over-Constrained Payoff: Vector Meson Truncation (P-wave only)

Kinematic Setup	Amps	Real Params	Moments/SDMEs	Physical Impact
Unpolarized	9	16	23	<i>Allows single-energy <math>L/T</math> separation</i>
Single-Polarized	18	35	94	<i>Also full separation into <math>k</math>-amplitudes</i>
Double-Polarized	18	35	376	<i>Also full separation into <math>k</math>-amplitudes</i>

# Equivalence to Previous Work

In the limit we restrict our partial wave content to  $J=1$ , this formalism should be equivalent to previous amplitude formalisms

Vector meson production from a polarized nucleon

Markus Diehl

Published 17 September 2007 • Published under licence by IOP Publishing Ltd

[Journal of High Energy Physics, Volume 2007, JHEP09\(2007\)](#)

Citation Markus Diehl JHEP09(2007)064

DOI 10.1088/1126-6708/2007/09/064

Home > The European Physical Journal C > Article

## Ratios of helicity amplitudes for exclusive $\rho^0$ electroproduction on transversely polarized protons

The HERMES Collaboration

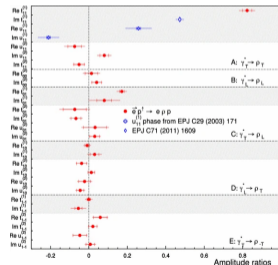
Regular Article - Experimental Physics | [Open access](#) | Published: 08 June 2017

Volume 77, article number 378 (2017) | [Cite this article](#)

## New

Our formalism naturally extends to

- Any and mixed  $J$  (for spectroscopy)
- Polarised recoil (e.g. for  $K^* \Lambda$ )
- Defines moments as model independent data summary. (Up to some  $L_{max}$ )
- Further extendable to final states other than 2 spin0 decay.



# Modelling Vector Meson Production with Regge

PHYSICAL REVIEW D 97, 094003 (2018)

## Vector meson photoproduction with a linearly polarized beam

V. Mathieu,<sup>1,\*</sup> J. Nys,<sup>1,2,3,4</sup> C. Fernández-Ramírez,<sup>5</sup> A. Jackura,<sup>3,4</sup>  
A. Piloni,<sup>1</sup> N. Sherrill,<sup>3,4</sup> A. P. Szczepaniak,<sup>1,3,4</sup> and G. Fox<sup>6</sup>

(Joint Physics Analysis Center)

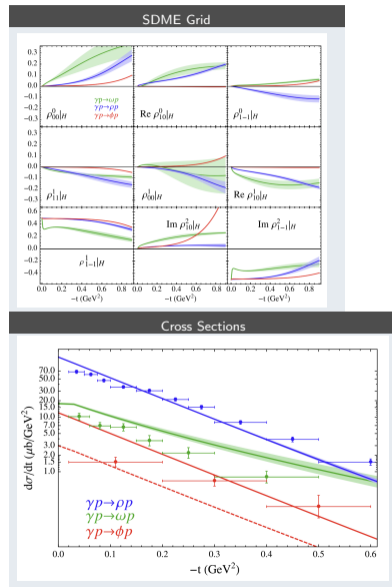
## Regge Trajectory Classification

	Non-Flip ( $k = +1$ )	Spin-Flip ( $k = -1$ )
<b>Natural</b> ( $\epsilon = +1$ )	Pomeron ( $\mathbb{P}$ ), $f_2$	$a_2$
<b>Unnatural</b> ( $\epsilon = -1$ )	$f_1, a_1$ (Neglected)	$\pi, \eta$ (Pseudoscalar)

## Core Modeling Principles

- **Vertex Factorization:** High-energy amplitudes factorize into independent photon ( $T^E$ ) and nucleon ( $B^E$ ) vertices linked by a Regge propagator  $R^E(s, t)$ .
- **Nucleon Constraints:** Isoscalar natural exchanges ( $\mathbb{P}, f_2$ ) are empirically nucleon helicity non-flip, while the isovector  $a_2$  dominates nucleon spin-flip currents.
- **Pseudoscalar Saturation:** Unnatural exchanges are saturated by active  $\pi$  and  $\eta$  trajectories, leaving charge-conjugation constraints to force a pure nucleon spin-flip structure.
- **Application:** Provides amplitude level calculations

Plan to refine with new GlueX data  
and extend to  $Q^2$  with CLAS12 data.



# Summary and Outlook

## Key Framework Objectives

- **Model Independence I:** Experimental data can be completely summarised by Polarised Spherical Harmonic moments  $H^\alpha(LM)$ .
- **Unpolarised Experiments:** Relating these moments to underlying partial wave amplitudes of any contributing meson resonances reduces number of independent parameters.
- **Polarised nucleons:** We generalised to polarised nucleons, doubling the measurable amplitudes.
- **L/T separation** Restricting the model dependence to Regge factorisation allows Single Energy L/T separations. In principle polarised nucleon experiments allow fully model independent extractions.

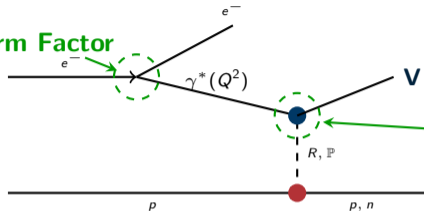
## Current Status & Next Steps

- **Formalism:** paper write up in progress.
- **Tools:**
  - Moment to amplitude inverter developed.
  - Moment fitting tools for electro-production under-development.
  - Inclusive Generator based on JPAC models under-development.

**Conclusion: Methods developed for complex amplitude analysis in photoproduction for Hadron Spectroscopy experiments are ready to be implemented in electro-production reactions.**

# Electroproduction Event Generator : eSpectro - CLAS12/EIC

Virtual Photon Flux + Form Factor



Photoproduction Amplitudes  
→ from jpacPhoto  
(Regge + VMD)

## 4-Fold Differential Cross Section Factorization

$$\frac{d^4\sigma}{ds dQ^2 d\phi dt} = \frac{d^2\sigma_{e,\gamma^*e'}}{ds dQ^2} \times \frac{d^2\sigma_{\gamma^*+p \rightarrow V+p}(s, Q^2)}{d\phi dt}$$

## Kinematic Dictionary

$$L = \frac{1 + (1 - y)^2}{y} - \frac{2m_e^2 y}{Q^2}$$

$$K = \frac{W^2 - M^2}{2M} = \nu(1 - x) = Ey(1 - x) = \nu - \frac{Q^2}{2M}$$

## Virtual Photon Flux Component

$$\frac{d^2\sigma_{e,\gamma^*e'}}{ds dQ^2} = \frac{\alpha}{2\pi} \cdot \frac{K \cdot L}{E} \cdot \frac{1}{Q^2} \cdot \frac{1}{(s - M^2 + Q^2)}$$

## Physical Flux Trajectory

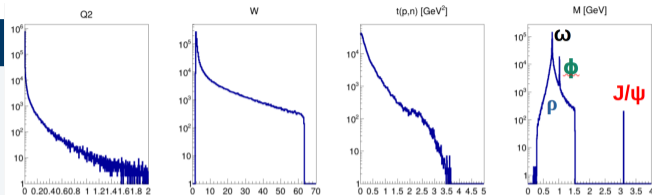
Photon flux rises rapidly as:

$Q^2 \rightarrow 0$  ;  $W = \sqrt{s} \rightarrow M_{\text{proton}}$   
→ Drives highly elevated production rates.

# Inclusive Vector Production Generator

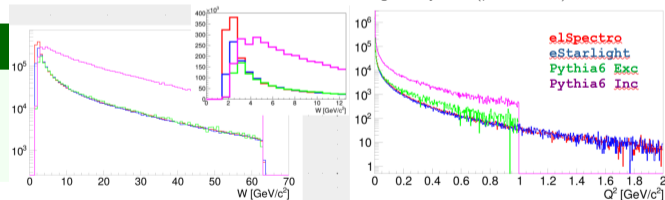
## Generator Pipeline Architecture

- **Hadronic Baseline:** Dynamically calculates transverse cross sections ( $\sigma_T$ ) by wrapping the core JPAC Regge photoproduction model amplitudes.
- **Low- $Q^2$  Optimization:** Sets longitudinal components ( $\sigma_L = 0$ ), providing a clean, high-speed framework tailored for quasi-real electroproduction tracking.
- **Flux Convolution:** Integrates the differential cross sections directly against the virtual photon flux to define total yields, sampling phase-space event generation proportionally.



Generated inclusive production profiles tracking the clear  $\rho$ ,  $\omega$ ,  $\phi$ , and  $J/\psi$  mass states.

## Generator Validation vs. eStarlight & Pythia6 ( $\rho$ Production)



$Q^2$  Scaling Comparison

Hadronic Invariant Mass  $W$

## Decay & Polarization Physics

- **Branching Channels:** Opens all native vector meson decay branches to track full multi-pion and kaon final-state kinematics.
- **Anisotropic Distributions:** Generates explicit decay angular topologies directly weighted by the calculated spin density matrix elements (SDMEs).

# Generalization to Polarized Target and Recoil

The macroscopic cross section expands systematically to include polarized initial targets ( $\beta \in \{1, 2, 3\}$ ) and recoils ( $\delta \in \{1, 2, 3\}$ ). We do not need a new normalization scheme; **the unpolarized scale factor ( $\mathcal{N}$ ) anchors the entire polarized density matrix.**

## Fully Polarized Macroscopic Cross Section

$$\frac{d^5\sigma(\mathbf{S}_I, \mathbf{S}_R)}{dQ^2 dW dt dm d\Phi} = \Gamma(Q^2, W) \sum_{\alpha=0}^8 \sum_{\beta=0}^3 \sum_{\delta=0}^3 P_{\alpha\beta\delta}(\Phi, \mathbf{S}_I, \mathbf{S}_R) \frac{d^2\sigma^{\alpha\beta\delta}}{dt dm}$$

$$\text{Extraction Recipe: } \sigma^{\alpha\beta\delta} = \mathcal{N} \cdot \hat{H}^{\alpha\beta\delta}(00)$$

## Activation of Imaginary Structure Functions ( $A_{UT}, A_{LL}$ )

The imaginary interference responses ( $\alpha \in \{2, 3, 6, 7\}$ ) strictly require a total parity product of  $S_\alpha \tau_\beta \tau_\delta = +1$  to survive mathematically.

### Case Study: Target Single-Spin Asymmetry ( $A_{UT}^{\sin\Phi}$ )

When an unpolarized beam ( $\alpha = 6, S_6 = -1$ ) strikes a target polarized normal to the scattering plane ( $\beta = 2, \tau_2 = -1$ ), the parity signs compensate:

$$(-1)_{S_\alpha} \times (-1)_{\tau_\beta} \times (+1)_{\tau_\delta} = +1$$

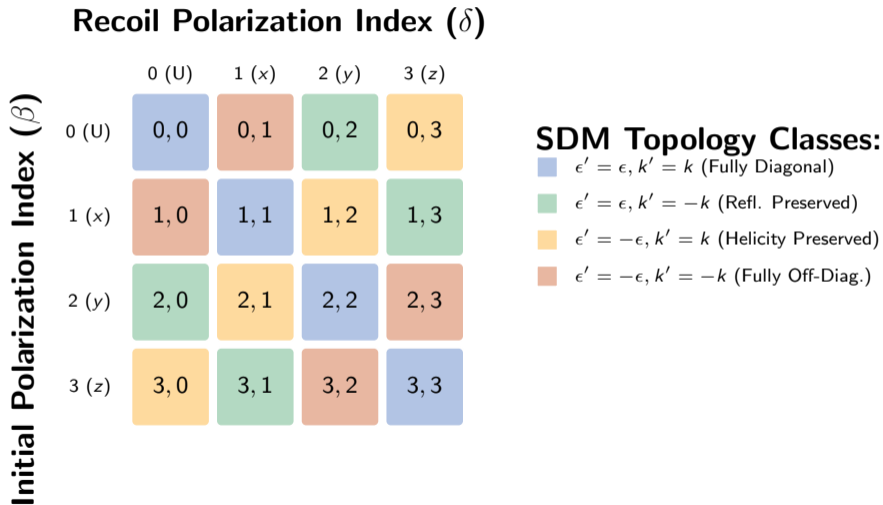
This activates the scalar moment  $H^{620}(00)$ , producing the target SSA cross section:

$$\frac{d^2\sigma_{LT}^{\sin\Phi, y}}{dt dm} = \mathcal{N} \cdot \hat{H}^{620}(00)$$

*The  $k$ -basis formalism mathematically mandates which observables require nucleon polarization to become experimentally accessible.*

# SDM Topology: Initial–Recoil Polarization Mapping

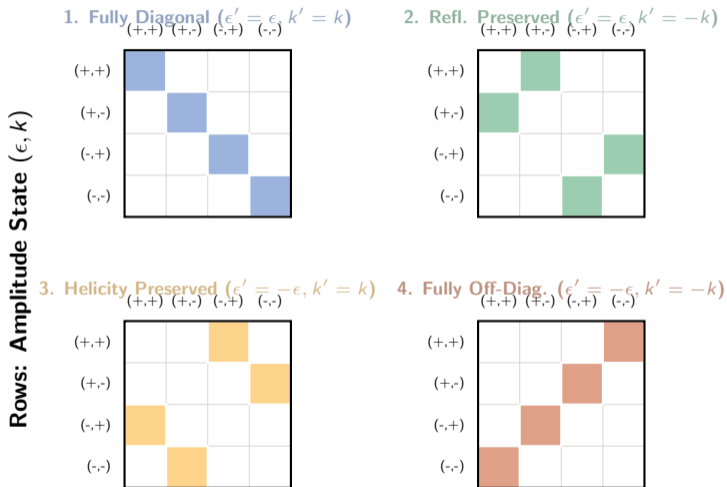
Pick a polarised experiment :



Note:  $\beta + \delta = \text{even}$  (Blue/Green) isolates block-diagonal reflectivity elements;  $\beta + \delta = \text{odd}$  (Yellow/Red) isolates the naturality-interference cross-terms.

# Spin Density Matrix: Interference Projections

Columns: Conjugated State ( $\epsilon', k'$ )



- **Diagonal Classes (1, 2):** Map intensities and nucleon-spin interference within fixed exchange naturalities.
- **Off-Diagonal Classes (3, 4):** Isolate interference between Natural and Unnatural exchange parities.

# Inside the $(\epsilon, k)$ Matrix

By zooming in on the  $4 \times 4$  matrix, we can see exactly how the exchange naturality ( $\epsilon$ ) and the nucleon helicity ( $k$ ) map to specific physical interference terms.

**Natural** ( $\epsilon' = +$ ) **Unnatural** ( $\epsilon' = -$ )

		$k = +$	$k = -$	$k = +$	$k = -$
<b>Natural</b> ( $\epsilon = +$ )  <b>Unnatural</b> ( $\epsilon = -$ )	$k = +$	Non-Flip	Flip Interfere	Reflectivity Interference	
	$k = -$	Flip Interfere	Flip		
	$k = +$	Reflectivity Interference		Pure Unnatural	
	$k = -$				

## General Sub-Matrix Dimensions

Each cell represents an interference block of amplitudes  $[\ell]_{Xm;k}^\epsilon$ . The number of elements inside each block depends on the allowed partial waves ( $\ell, m$ ) and photon states ( $X \in \{L, T\}$ ).

- **Natural Amps ( $N^+$ ):** Contains all allowed Transverse and Longitudinal partial waves.
- **Unnatural Amps ( $N^-$ ):** Contains strictly fewer states than  $N^+$ , because the unnatural Longitudinal  $L_{m=0}$  state vanishes analytically due to parity conservation.

## Case Study: Vector Meson ( $\ell = 1$ )

For a vector meson, the 9 partial waves per  $k$ -sector split asymmetrically:

- **Natural ( $N^+ = 5$ ):**  $T_1, T_0, T_{-1}, L_1, L_0$
- **Unnatural ( $N^- = 4$ ):**  $T_1, T_0, T_{-1}, L_1$

Consequently, the intersecting cells form heterogeneously sized matrices:

- **Pure Natural:**  $N^+ \times N^+ = 5 \times 5$  sub-matrix
- **Parity Interf.:**  $N^+ \times N^- = 5 \times 4$  sub-matrix
- **Pure Unnatural:**  $N^- \times N^- = 4 \times 4$  sub-matrix

# Electroproduction Formalism VII: Polarized Target and Recoil

Activating initial target ( $\beta > 0$ ) or final recoil ( $\delta > 0$ ) polarization breaks the  $k$ -degeneracy. The Pauli spin matrices ( $\sigma^\beta, \sigma^\delta$ ) act as mathematical operators, explicitly coupling the nucleon helicity transitions ( $k'$  and  $k$ ):

## Generalized Polarized Response Blocks

**Pure Transverse Example ( $\alpha = 0$ ):**

$$\rho_{mm'}^{0\beta\delta} = \frac{\kappa}{2} \sum_{k', k, \epsilon} \langle k' | \sigma^\beta \sigma^\delta | k \rangle \left( [\ell]_{Tm; k'}^\epsilon [\ell']_{Tm'; k}^{\epsilon*} \right. \\ \left. + (-1)^{m' - m} [\ell]_{T, -m; k'}^\epsilon [\ell']_{T, -m'; k}^{\epsilon*} \right)$$

**Pure Longitudinal Example ( $\alpha = 4$ ):**

$$\rho_{mm'}^{4\beta\delta} = \kappa \sum_{k', k, \epsilon} \langle k' | \sigma^\beta \sigma^\delta | k \rangle \left( [\ell]_{Lm; k'}^\epsilon [\ell']_{Lm'; k}^{\epsilon*} \right)$$

**Longitudinal-Transverse Example ( $\alpha = 5$ ):**

$$\rho_{mm'}^{5\beta\delta} = \frac{\kappa}{2\sqrt{2}} \sum_{k', k, \epsilon} \langle k' | \sigma^\beta \sigma^\delta | k \rangle \left( [\ell]_{Lm; k'}^\epsilon [\ell']_{Tm'; k}^{-\epsilon*} \right. \\ \left. + [\ell]_{Tm; k'}^\epsilon [\ell']_{Lm'; k}^{-\epsilon*} \pm \dots \right)$$

## The Spin Filter: Isolating the Physics

The operator  $\langle k' | \sigma^\beta \sigma^\delta | k \rangle$  acts as a strict selector switch for the interference topologies.

**1. Unpolarized ( $\beta = 0, \delta = 0$ ):**  $\sigma^0 = \mathbb{I}$   
Forces  $k' = k$ . The sums collapse to  $\sum_k A_k A_k^*$ . Non-flip and flip transitions cannot interfere.

**2. Transverse Target ( $\beta = 2$ ):**  $\sigma^2 = \sigma_y$   
The Pauli-y matrix is off-diagonal. It strictly forces  $k' = -k$ . The response entirely isolates the interference between nucleon non-flip ( $k = +1$ ) and spin-flip ( $k = -1$ ) amplitudes.

**3. Longitudinal Target ( $\beta = 3$ ):**  $\sigma^3 = \sigma_z$   
The Pauli-z matrix is diagonal. It forces  $k' = k$  but applies a relative sign difference (+1 for  $k = +1$ , -1 for  $k = -1$ ).

**Phenomenological Rule:** Target/Recoil polarization does not alter the photon reflectivity ( $\epsilon$ ) couplings; it exclusively unlocks the hidden nucleon helicity ( $k$ ) interferences.

# Electroproduction Formalism: The 9 Response Categories

Expanding the unpolarized system in this reduced  $k$ -basis explicitly isolates the 9 independent virtual-photon response blocks from same-reflectivity bilinears. Structures are identical for  $\beta, \delta \neq 0$ :

## Pure Transverse Response Blocks ( $\alpha = 0, 1, 2, 3$ )

$$\begin{aligned}\rho_{mm'}^{0,\ell\ell'} &= \frac{\kappa}{2} \sum_{k,\epsilon} \left( [\ell]_{Tm;k}^{\epsilon} [l']_{Tm';k}^{\epsilon*} + (-1)^{m'} - m [\ell]_{T,-m;k}^{\epsilon} [l']_{T,-m';k}^{\epsilon*} \right) \\ \rho_{mm'}^{1,\ell\ell'} &= -\frac{\kappa}{2} \sum_{k,\epsilon} \epsilon \left( (-1)^m [\ell]_{T,-m;k}^{\epsilon} [l']_{Tm';k}^{\epsilon*} + (-1)^{m'} [\ell]_{Tm;k}^{\epsilon} [l']_{T,-m';k}^{\epsilon*} \right) \\ \rho_{mm'}^{2,\ell\ell'} &= -\frac{i\kappa}{2} \sum_{k,\epsilon} \epsilon \left( (-1)^m [\ell]_{T,-m;k}^{\epsilon} [l']_{Tm';k}^{\epsilon*} - (-1)^{m'} [\ell]_{Tm;k}^{\epsilon} [l']_{T,-m';k}^{\epsilon*} \right) \\ \rho_{mm'}^{3,\ell\ell'} &= \frac{\kappa}{2} \sum_{k,\epsilon} \left( [\ell]_{Tm;k}^{\epsilon} [l']_{Tm';k}^{\epsilon*} - (-1)^{m'} - m [\ell]_{T,-m;k}^{\epsilon} [l']_{T,-m';k}^{\epsilon*} \right)\end{aligned}$$

## Pure Longitudinal Response Block ( $\alpha = 4$ )

$$\rho_{mm'}^{4,\ell\ell'} = \kappa \sum_{k,\epsilon} [\ell]_{Lm;k}^{\epsilon} [l']_{Lm';k}^{\epsilon*}$$

## Longitudinal-Transverse Interferences ( $\alpha = 5, 6, 7, 8$ )

$$\begin{aligned}\rho_{mm'}^{5,\ell\ell'} &= \frac{\kappa}{2\sqrt{2}} \sum_{k,\epsilon} \left( [\ell]_{Lm;k}^{\epsilon} [l']_{Tm';k}^{-\epsilon*} + [\ell]_{Tm;k}^{\epsilon} [l']_{Lm';k}^{-\epsilon*} \right. \\ &\quad \left. + (-1)^{m'} - m ([\ell]_{L,-m;k}^{\epsilon} [l']_{T,-m';k}^{-\epsilon*} + [\ell]_{T,-m;k}^{\epsilon} [l']_{L,-m';k}^{-\epsilon*}) \right) \\ \rho_{mm'}^{6,\ell\ell'} &= -\frac{\kappa}{2\sqrt{2}} \sum_{k,\epsilon} \left( [\ell]_{Lm;k}^{\epsilon} [l']_{Tm';k}^{-\epsilon*} + [\ell]_{Tm;k}^{\epsilon} [l']_{Lm';k}^{-\epsilon*} \right. \\ &\quad \left. + (-1)^{m'} - m ([\ell]_{L,-m;k}^{\epsilon} [l']_{T,-m';k}^{-\epsilon*} + [\ell]_{T,-m;k}^{\epsilon} [l']_{L,-m';k}^{-\epsilon*}) \right) \\ \rho_{mm'}^{7,\ell\ell'} &= \frac{\kappa}{2\sqrt{2}} \sum_{k,\epsilon} \left( [\ell]_{Lm;k}^{\epsilon} [l']_{Tm';k}^{-\epsilon*} + [\ell]_{Tm;k}^{\epsilon} [l']_{Lm';k}^{-\epsilon*} \right. \\ &\quad \left. - (-1)^{m'} - m ([\ell]_{L,-m;k}^{\epsilon} [l']_{T,-m';k}^{-\epsilon*} + [\ell]_{T,-m;k}^{\epsilon} [l']_{L,-m';k}^{-\epsilon*}) \right) \\ \rho_{mm'}^{8,\ell\ell'} &= \frac{\kappa}{2\sqrt{2}} \sum_{k,\epsilon} \left( [\ell]_{Lm;k}^{\epsilon} [l']_{Tm';k}^{-\epsilon*} - [\ell]_{Tm;k}^{\epsilon} [l']_{Lm';k}^{-\epsilon*} \right. \\ &\quad \left. + (-1)^{m'} - m ([\ell]_{L,-m;k}^{\epsilon} [l']_{T,-m';k}^{-\epsilon*} - [\ell]_{T,-m;k}^{\epsilon} [l']_{L,-m';k}^{-\epsilon*}) \right)\end{aligned}$$

**Symmetry Rule:** Pure  $T$  and  $L$  blocks sum over identical reflectivities ( $\epsilon$ ), while cross-talk  $LT$  components step anti-diagonally via ( $\epsilon \cdot -\epsilon$ )